Handout # 15 (MEEN 617) **Application example**

Experimental identification of bearing force coefficients

Consider a test bearing or seal element as a point mass undergoing forced vibrations induced by external forcing functions. The equations of motion for small amplitudes about an equilibrium position are described in linear form as,

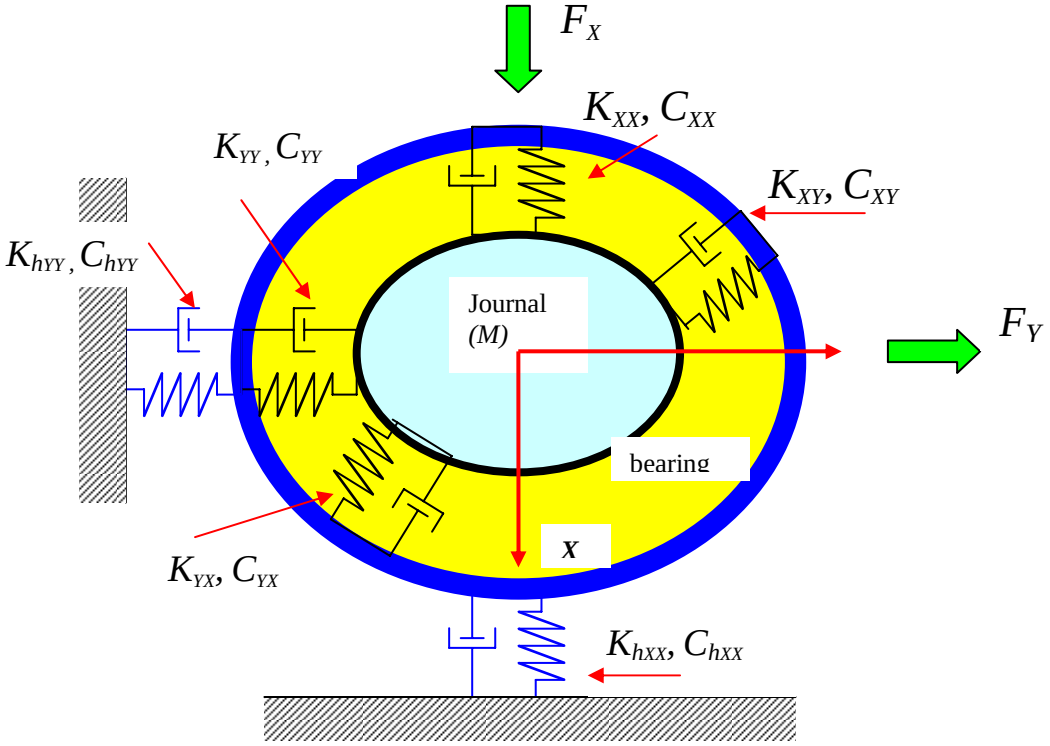

Representation of point mass and bearing force coefficients used for identification of parameters from dynamic load and motion measurements

$$M_h\ddot{x} + \left(C_{XX} + C_{hX}\right)\dot{x} + C_{XY}\dot{y} + \left(K_{XX} + K_{hX}\right)x + K_{XY}y = f_X$$

$$M_h\ddot{y} + \left(C_{YY} + C_{hY}\right)\dot{y} + C_{YX}\dot{x} + \left(K_{YY} + K_{hY}\right)y + K_{YX}x = f_Y \qquad (1)$$

where $\{f_i\}_{i=X,Y}$ are external excitation forces, M_h is the test element mass, $\{K_{hi},C_{hi}\}_{i=X,Y}$ are structural support stiffness and damping coefficients, and $\{K_{ij},C_{ij}\}_{i,j=X,Y}$ are the seal/bearing dynamic stiffness and damping force coefficients, respectively. Inertia force coefficients are not accounted for in the model above. These coefficients are insignificant for highly compressible fluids (LH2 or air) and for most bearing applications with mineral lubricants. This apparent simplification is easily removed and does not diminish the importance of the identification method.

The structural stiffness and damping coefficients, $\{K_{hi},C_{hi}\}_{i=X,Y}$, are obtained from prior shake results under dry conditions, i.e. without fluid through the test element

Two independent forced excitations (impact, periodic-single frequency, sine-swept, random, etc) $(f_X,0)^T$ and $(0,f_Y)^T$, for example, are applied to the test element. This process can be written as:

1. Apply $\begin{bmatrix} f_{x_1} \\ f_{y_1} \end{bmatrix}_{(t)}$ and measure $\begin{bmatrix} x_{1_{(t)}} \\ y_{1_{(t)}} \end{bmatrix}$ (2a)

2. Apply $\begin{bmatrix} f_{x_2} \\ f_{y_2} \end{bmatrix}_{(t)}$ and measure $\begin{bmatrix} x_{2_{(t)}} \\ y_{2_{(t)}} \end{bmatrix}$ (2b)

3. Obtain the **discrete Fourier transform (FFT)** of the applied forces and displacements, i.e. Let

$$\begin{bmatrix} F_{X_{1(\omega)}} \\ F_{Y_{1(\omega)}} \end{bmatrix} = FFT \begin{bmatrix} f_{x_{1(t)}} \\ f_{Y_{1(t)}} \end{bmatrix}; \begin{bmatrix} X_{1(\omega)} \\ Y_{1(\omega)} \end{bmatrix} = FFT \begin{bmatrix} x_{1(t)} \\ y_{1(t)} \end{bmatrix};$$
$$\begin{bmatrix} F_{X_{2(\omega)}} \\ F_{Y_{2(\omega)}} \end{bmatrix} = FFT \begin{bmatrix} f_{x_{2(t)}} \\ f_{Y_{2(t)}} \end{bmatrix}; \begin{bmatrix} X_{2(\omega)} \\ Y_{2(\omega)} \end{bmatrix} = FFT \begin{bmatrix} x_{2(t)} \\ y_{2(t)} \end{bmatrix} \quad (2b)$$

The FFT is an operation that transforms the information from the **time domain** into the **frequency domain**. Incidentally, recall that

$$i\,\omega\, X_{(\omega)} = FFT\left[\dot{x}_{(t)}\right];\quad -\omega^2\, X_{(\omega)} = FFT\left[\ddot{x}_{(t)}\right] \tag{2c}$$

4. For the assumed physical model, the equations of motion in the frequency domain become,

$$-M_h\omega^2\, X_1 + \left(C_{XX} + C_{hX}\right) i\omega X_1 + C_{XY} i\omega Y_1 + \left(K_{XX} + K_{hX}\right) X_1 + K_{XY} Y_1 = F_{X_1} \tag{2d}$$

$$-M_h\omega^2\, Y_1 + \left(C_{YY} + C_{hY}\right) i\omega Y_1 + C_{YX} i\omega X_1 + \left(K_{YY} + K_{hY}\right) Y_1 + K_{YX} X_1 = F_{Y_1} \tag{2e}$$

Or, written in matrix form as

$$\begin{bmatrix} K_{XX} + K_{hX} - M_h\omega^2 + i\omega\left(C_{XX} + C_{hX}\right) & K_{XY} + i\omega C_{XY} \\ K_{YX} + i\omega C_{YX} & K_{YY} + K_{hY} - M_h\omega^2 + i\omega\left(C_{YY} + C_{hY}\right) \end{bmatrix} \begin{Bmatrix} X_1 \\ Y_1 \end{Bmatrix} = \begin{Bmatrix} F_{X_1} \\ F_{Y_1} \end{Bmatrix} \tag{3}$$

Define **complex impedances**[1] $\{H_{ij}\}_{i,j=X,Y}$ as

$$H_{ij} = \left[\left(K_{ij} + K_{hi}\delta_{ij}\right) - \omega^2 M_{hi}\delta_{ij}\right] + i\omega\left(C_{ij} + C_{hi}\delta_{ij}\right) \tag{4}$$

where $i = \sqrt{-1}$, $\delta_{ij} = 1$ for $i = j = X, Y$; zero otherwise. The impedances are composed of real and imaginary parts, both functions of frequency (ω). The real part denotes the dynamic stiffness, while the imaginary part

[1] This is, as you know, a misnomer. Dynamic (complex) stiffness is a more appropriate name.

(quadrature stiffness) is proportional to the *viscous* damping coefficient, as shown in the figure below.

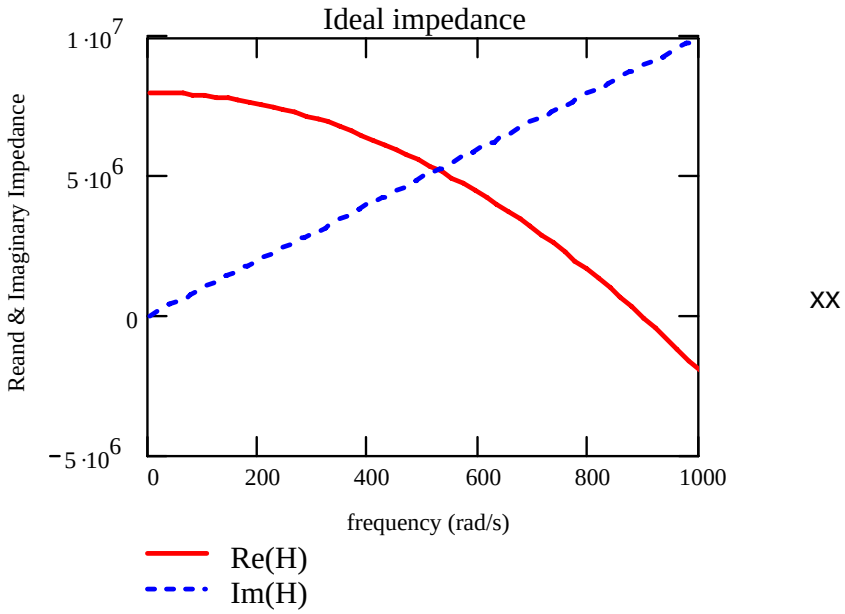

Real and imaginary parts of ideal mechanical impedance

With definition (4), the EOMs (3) become, for the first measurement,

$$\begin{bmatrix} H_{XX_{(\omega)}} & H_{XY_{(\omega)}} \\ H_{YX_{(\omega)}} & H_{YY_{(\omega)}} \end{bmatrix} \begin{Bmatrix} X_1 \\ Y_1 \end{Bmatrix} = \begin{Bmatrix} F_{X_1} \\ F_{Y_1} \end{Bmatrix} \tag{5a}$$

And similarly, for the second test,

$$\begin{bmatrix} H_{XX_{(\omega)}} & H_{XY_{(\omega)}} \\ H_{YX_{(\omega)}} & H_{YY_{(\omega)}} \end{bmatrix} \begin{Bmatrix} X_2 \\ Y_2 \end{Bmatrix} = \begin{Bmatrix} F_{X_2} \\ F_{Y_2} \end{Bmatrix} \tag{5b}$$

Add these two equations gives and reorganize them as (Robison et al., 1995),

$$\begin{bmatrix} X_1 & Y_1 \\ X_2 & Y_2 \end{bmatrix} \begin{bmatrix} H_{XX} & H_{YX} \\ H_{XY} & H_{YY} \end{bmatrix} = \begin{bmatrix} F_{X_1} & F_{Y_1} \\ F_{X_2} & F_{Y_2} \end{bmatrix} \quad (6)$$

Equation (6) represents **four independent equations** with **four unknowns**, $(H_{ij})_{i,,j=X,Y}$, easily found using Cramers' rule, for example, or

$$\begin{bmatrix} H_{XX} & H_{YX} \\ H_{XY} & H_{YY} \end{bmatrix} = \begin{bmatrix} X_1 & Y_1 \\ X_2 & Y_2 \end{bmatrix}^{-1} \begin{bmatrix} F_{X_1} & F_{Y_1} \\ F_{X_2} & F_{Y_2} \end{bmatrix} \quad (*)$$

The meaning of linear independence of the test forces (and ensuing motions) should now be clear. That is, the forces in the second test cannot just be a multiple of the first set of forces since then, the matrices of displacements and forces would be **singular**. IN general, the experimenter has to chose sets of excitations that are linearly independent, for example $(f_X,0)^T$ and $(0,f_Y)^T$ are preferred choices.

Preliminary estimates of the system parameters $\{M,\ K,\ C\}_{i,j=X,Y}$ are determined by curve fitting of discrete impedances $\{H_{ij}\}$ to the test data over a pre-selected frequency range. Rouvas and Childs (1993) use this impedance identification method exclusively for identification of force coefficients in hydrostatic bearings and seals with water as the lubricant.

System transfer functions (output/input) could be used to obtain more precise estimates of the seal/bearing force coefficients (Nordmann and Schollhorn, 1980, Massmann and Nordmann, 1985).

In terms of the impedances, $(H_{ij})_{i,,j=X,Y}$, the transfer functions describing system flexibilities are generated by the following equations:

$$G_{XX} = TF(X_1) = \frac{H_{YY}}{\Delta} \qquad G_{XY} = TF(X_2) = \frac{-H_{XY}}{\Delta}$$

$$G_{YX} = TF(Y_1) = \frac{-H_{YX}}{\Delta} \qquad G_{YY} = TF(Y_2) = \frac{H_{XX}}{\Delta} \qquad (7)$$

where $\Delta = H_{XX} H_{YY} - H_{XY} H_{YX}$.

Next, the **Instrumental Variable (IV) method** of Fritzen (1985), an extension of a **least-squares estimation** method, is used to simultaneously curve fit all four transfer functions from measurements in two orthogonal directions. **The method has the advantage of eliminating bias typically seen in an estimator due to measurement noise.**

The product of the flexibility (**G**) and impedance (**H**) matrices should be identically equal to the identity matrix since $\mathbf{G}=\mathbf{H}^{-1}$. However, in any measurement process there is some noise associated with the experimental measurements. Thus, an **error matrix** (**N**) is introduced into the relationship,

$$\mathbf{G} \cdot \mathbf{H} = \mathbf{G}\left[\mathbf{K} - \omega^2 \mathbf{M} + i\omega \mathbf{C}\right] = \mathbf{I} + \mathbf{N} \qquad (8)$$

where **K, M** and **C** are the matrices of system stiffness, mass and damping coefficients. Rearranged, this equation becomes

$$\mathbf{A} \begin{bmatrix} \mathbf{K} \\ \mathbf{M} \\ \mathbf{C} \end{bmatrix} = \mathbf{I} + \mathbf{N} \qquad (9)$$

where **A** contains the measured transfer functions. Solution of Eq. (9) by least-squares requires minimization of the loss function defined by the Euclidean norm of **N**. This minimization leads to the normal equations,

$$\mathbf{A}^T\mathbf{A}\begin{bmatrix}\mathbf{K}\\ \mathbf{M}\\ \mathbf{C}\end{bmatrix} = \mathbf{A}^T\mathbf{I} \qquad (10)$$

A first set of force coefficients is determined from these equations. Using the **IV** method extension, the weighting function, $\mathbf{A}^T$, is replaced by a new matrix function, $\mathbf{W}^T$, created from analytical transfer functions resulting from the initial least-squares curve fit. **This weighting function is free of measurement noise** and contains a peak only at the resonant frequency as determined from the first estimates of stiffness, mass and damping coefficients. The calculation cycle is continued until correlation is within a desired tolerance (Ransom, 1997).

Note that the stiffness and damping coefficients are identified in the frequency domain. Thus, magnitudes of uncertainty for the estimated force coefficients must be obtained by comparing the original frequency responses with the frequency response of a reference excitation force and associated displacement time response. Evaluation of coherence functions then becomes necessary to reproduce the exact variability of the identified force coefficients. Ransom (1997) describes at length the frequency domain uncertainty analysis implemented. Diaz and San Andrés (1999) provide in full a description of the identification method along with a MATHCAD program which allows the fast estimation of system parameters in real time.

Closure

Read the paper of Diaz and San Andrés (1999) – following pages- for further insight on experimental methods and identification procedures in bearings and seals. A MATHCAD program is available for your self-study and further learning.

References

Diaz, S., and L. San Andrés, 1999, "A Method for Identification of Bearing Force Coefficients and its Application to a Squeeze Film Damper with a Bubbly Lubricant," STLE Tribology Transactions, Vol. 42, 4, pp. 739-746, (STLE Paper 99-AM-5).

Fritzen, C. P., 1985, "Identification of Mass, Damping, and Stiffness Matrices of Mechanical Systems," ASME Paper 85-DET-91.

Massmann, H., and R. Nordmann, 1985, "Some New Results Concerning the Dynamic Behavior of Annular Turbulent Seals," Rotordynamic Instability Problems of High Performance Turbomachinery, Proceedings of a workshop held at Texas A&M University, Dec, pp. 179-194.

Nordmann, R., and K. Schollhorn, 1980, "Identification of Stiffness and Damping Coefficients of Journal Bearings by Means of the Impact Method," Proceedings of the 2nd International Conference on Vibrations in Rot. Mach., IMechE, pp.231-238.

Ransom, D. L., 1997, "Identification of Dynamic Force Coefficients of a Labyrinth and Gas Damper Seals Using Impact Load Excitations," Master's Thesis, Texas A&M University, December.

Robison, M, G. Arauz, and L. San Andrés, 1995, "A Test Rig for the Identification of Rotordynamic Force Coefficients of Fluid Film Bearing Elements," ASME Paper 95-GT-431.

Rouvas, C., and D. Childs, 1993, "A Parameter Identification Method for the Rotordynamic Coefficients of a High Speed Reynolds Number Hydrostatic Bearing," ASME *Journal of Vibration and Acoustics*, Vol. 115, pp. 264-270.

Vol. 42 (1999), 4, 739-746
TRIBOLOGY TRANSACTIONS

A Method for Identification of Bearing Force Coefficients and Its Application to a Squeeze Film Damper with a Bubbly Lubricant©

SERGIO E. DIAZ and LUIS A. SAN ANDRÉS (Member, STLE)
Texas A&M University
Mechanical Engineering Department
College Station, Texas 77843

A general formulation of the instrumental variable filter (IVF) method for parameter identification of a n-DOF (Degrees Of Freedom) mechanical linear system is presented. The IVF is a frequency domain method and an iterative variation of the least-squares approximation to the system flexibilities. Weight functions constructed with the estimated flexibilities are introduced to reduce the effect of noise in the measurements, thus improving the estimation of dynamic force coefficients. The IVF method is applied in conjunction to impact force excitations to estimate the mass, stiffness, and damping coefficients of a test rotor supported on a squeeze film damper (SFD) operating with a bubbly lubricant. The amount of air in the lubricant is varied from nil to 100 percent to simulate increasing degrees of severity of air entrainment into the damper film lands. The experimental results and parameter estimation technique show that the SFD damping force coefficients increase as the air volume fraction in the mixture increases to about 50 percent in volume content. The damping coefficients decrease rapidly for mixtures with larger air concentrations. The unexpected increase in direct damping coefficients indicates the complexity of the SFD bubbly flow field and warrants further experimental verification.

KEY WORDS

Squeeze-flim Lubrication; Dampers; Bearings

Presented at the 54th Annual Meeting
Las Vegas, Nevada
May 23-27, 1999
Final manuscript approved March 24, 1999

INTRODUCTION

Experimental identification of linearized bearing parameters, namely stiffness and damping force coefficients, is of importance to verify the rotordynamic performance of actual fluid film bear-

NOMENCLATURE

A	= matrix of coefficients for error equation [2nN,3n]
c	= SFD nominal radial clearance [0.290 mm]
C	= matrix of damping coefficients [nxn]
C_{ij}	= equivalent damping coefficients of SFD-rotor system [Nsec/m]
d	= shaft diameter [9.5 mm]
D	= journal diameter [50.8 mm]
$\underline{E}$	= error matrix [n,n]
$\bar{E}$	= extended error matrix [2nN,n]
f	= forcing vector [n]
F	= DFT of the force vector f [n]
$\underline{F}$	= flexibility matrix [n,n]
$\underline{H}$	= impedance matrix [n,n]
i	= imaginary unit [$\sqrt{-1}$]
I	= identity matrix [n,n]
$\bar{I}$	= extended identity matrix [2nN,n]
i,j	= indexes for degrees of freedom [=1,2,...n]
k	= frequency index
K	= matrix of stiffness coefficients [n,n]
K_{ij}	= equivalent stiffness coefficients of SFD-rotor system [N/m]
l	= shaft length [304.8 mm]
L	= journal length [25.4 mm]
m	= iteration counter for IVF method
M	= matrix of inertia coefficients [n,n]
M_{ij}	= equivalent inertia coefficients of SFD-rotor system [kg]
n	= number of degrees of freedom of the system
N	= number of frequencies considered for identification range
t	= time [sec]
W	= weight matrix for IV method [2nN,3n]
x	= displacements (state) vector [n]
X	= DFT of the displacement vector x [n]
X, Y	= horizontal and vertical coordinates, respectively
μ	= fluid viscosity [Pa.s]
ω	= frequency [rad/s]
0	= zero (null) matrix [n,n]

ing elements and to validate (and calibrate) predictive tools for computation of bearing and seal dynamic forced responses. The ultimate goal is to provide reliable data bases from which to determine the confidence of bearing and/or seal operation under both normal design conditions and extreme environments due to unforeseen events. In addition, even advanced analytical models are very limited or non-existing for certain bearing and seal configurations and with stringent particular operating conditions, and thus experimental measurements of actual bearing force coefficients constitute the only option available to generate engineering results of interest. Squeeze film dampers operating with air entrainment are but an example of the many applications where systematic experimentation becomes mandatory.

The estimation of bearing and seal rotordynamic force coefficients has been traditionally based on time domain response procedures *(1)*. However, these techniques are limited in their scope, use only a limited amount of the recorded information, and often provide poor results with marginal confidence levels *(2)*. Modern bearing parameter identification techniques are based on frequency domain procedures, where dynamic force coefficients are estimated from transfer functions of measured displacements (velocities and accelerations as well) due to external loads of a prescribed time varying structure. The frequency domain methods take advantage of high speed computing and processors, thus producing estimates of system parameters in real time and at a fraction of the cost (and effort) prevalent with cumbersome time domain techniques *(3)-(5)*.

This paper presents a frequency domain method for identification of linearized bearing force coefficients from test fluid film bearing elements. The technique, a variation of a least square estimator, is based on the Instrumental Variable Filter (IVF) Method with the capability to automatically reduce the noise inherent in any measurement and to provide reliable bearing force coefficients within a frequency range. The analysis introduces the equations of motion for the test system and the measurement of time domain responses. The description follows with the transformation of displacement and load dynamic responses to the frequency domain, and the implementation of the procedure for error minimization and curve fitting of the (output/input) transfer functions over a selected frequency range.

The identification method is applied to the estimation of system force coefficients $/K_{ij}, C_{ij}, M_{ij}/_{ij=X,Y}$ for a small test rotor supported on a squeeze film damper (SFD). Calibrated impact guns excite the rotor in two radial planes *(X, Y)* and the rotor displacements are recorded for a multiple sequence of impacts. The SFD operates with an air in oil (bubbly) mixture to simulate prevalent operating conditions with air entrainment *(6)*. The identification procedure also renders dry, i.e. without lubricant, structural force coefficients.

INSTRUMENTAL VARIABLE PARAMETER IDENTIFICATION TECHNIQUE

Consider a n-degree of freedom linear mechanical system governed by the following system of differential equations.

$$M\ddot{x}_{(t)} + C\dot{x}_{(t)} + Kx_{(t)} = f_{(t)} \qquad [1]$$

where $f_{(t)}$ and $x_{(t)}$ represent the external forcing function and system displacements, respectively. The (•) denotes differentiation with respect to time. The square matrices *M, K* and *C* contain the generalized mass, stiffness and damping force coefficients representing the parameters of the system. The objective of the identification procedure is to determine the system force coefficients from measurements of the system dynamic response due to applied external loads. The governing equations can be written in the frequency domain as

$$\left[-\omega^2 M + i\omega C + K\right]X_{(\omega)} = \underline{H}_{(\omega)}X_{(\omega)} = F_{(\omega)} \qquad [2]$$

where $X_{(\omega)}$ and $F_{(\omega)}$ are the discrete Fourier transforms (DFT) of the time varying forces and displacements, $f_{(t)}$ and $x_{(t)}$, respectively. The impedance of the system is generally defined as

$$\underline{H}_{(\omega)} = \left[-\omega^2 M + i\omega C + K\right];\ i = \sqrt{-1} \qquad [3]$$

The n^2 impedance coefficients $\{\underline{H}_{i,j}\}_{i,j=1,\ldots n}$ are complex algebraic functions of the excitation frequency (ω). However, the system of Eq. [2] provides n equations for n^2 unknowns. A n-DOF (Degrees Of Freedom) system has n-linearly independent modes of vibration. Thus, n-linearly independent excitations $\{F^i\}_{i=1,\ldots n}$ should lead to n-linearly independent responses $\{X^i\}_{i=1,\ldots n}$, hence rendering n-linearly independent systems of equations of the form Eq. [2] for any given excitation frequency. The selection of the set of force excitations depends fundamentally on the structure and constraints of the system. A typical method consists of exciting the system at the location of each degree of freedom, one at the time . Note that this procedure when canned out with static loads leads naturally to the determination of the system flexibilities, i.e. the influence coefficient method. However, any combination of forcing functions is appropriate as long as the n-forces are linearly independent.

The n-systems of Eq. [2] representing the independent measurements can be regrouped in the following form,

$$\underline{H}_{(\omega)}\left[X^1_{(\omega)}\,\vdots\,X^2_{(\omega)}\,\vdots\,\mathrm{L}\,\vdots\,X^n_{(\omega)}\right] = \left[F^1_{(\omega)}\,\vdots\,F^2_{(\omega)}\,\vdots\,\mathrm{L}\,\vdots\,F^n_{(\omega)}\right] \qquad [4]$$

and the system impedance coefficients at the frequency of interest can be computed from

$$\underline{H}_{(\omega)} = \left[F^1_{(\omega)}\,\vdots\,F^2_{(\omega)}\,\vdots\,\mathrm{L}\,\vdots\,F^n_{(\omega)}\right]\left[X^1_{(\omega)}\,\vdots\,X^2_{(\omega)}\,\vdots\,\mathrm{L}\,\vdots\,X^n_{(\omega)}\right]^{-1} \qquad [5]$$

The definition of the impedance coefficients, Eq. [3], renders a quadratic relationship in frequency. To identify the force coefficients it is sufficient, in principle, to obtain the impedance coefficients at three different and well spaced frequencies and then use some curve-fit procedure to extract the force coefficients $(M_{i,j}, C_{i,j}, K_{i,j})_{i,j=1,2,\ldots,n}$. Note that the model assumes the force coefficients or system parameters are constants independent of frequency. In the following, the basic issues related to the selection of appropriate

test frequencies are discussed.

In a linear system excited by a sustained time varying force, the system response has the same frequency content as the external excitation as long as the transient motions not due to the external force have died out. Therefore, in an ideal case only pure-tone forced excitations are required, and response measurements conducted at only three different excitation frequencies should be sufficient to fully determine the system physical parameters. In practice, however, measurements of forces and displacements contain noise that affects greatly the desired results. In some other cases, the objective is to find linearized force coefficients that represent the behavior of a certain non-linear system over a frequency range. In both circumstances, whether dealing with measurement noise or localized system linearization, the identification procedure leads to a problem where the minimization of errors is of importance.

Instead of working with the minimum amount of frequencies needed, it is best to obtain measurements for a whole set of frequencies within a range of interest. However, an increased cost (and time) in the experimental procedure is the natural consequence if the measurements are conducted with a pure tone force excitation for every frequency of interest. Therefore, other forms of force excitations must be sought. The two excitations most commonly used are the impact load and the multi-harmonic force, though the sweep sine force is also often employed *(7)*.

The fundamental idea is to excite the system with a wide-band-spectrum force which will result in a wide-band system frequency response. The application of the DFT to the measured forces and displacements leads to discrete algebraic equations in the frequency domain and at the selected, say N, frequencies within the range of interest. The k^{th} impedance coefficients at the frequency (ω_k) could then be found from:

$$\underline{H}^k = \left[F^1_{(\omega_k)} \,\vdots\, F^2_{(\omega_k)} \,\vdots\, \cdots \,\vdots\, F^n_{(\omega_k)} \right] \left[X^1_{(\omega_k)} \,\vdots\, X^2_{(\omega_k)} \,\vdots\, \cdots \,\vdots\, X^n_{(\omega_k)} \right]^{-1}$$
$$k = 1,2,\ldots,N \qquad [6]$$

From here on, several paths could be followed to determine the $3n^2$ parameters $(M_{i,j},\ C_{i,j},\ K_{i,j})_{i,j=1,2,\ldots,n}$ from the n^2 impedance coefficients, $(\underline{H}_{i,j})_{i,j=1,2,\ldots,n}$ as functions of the excitation frequency. The most direct and most commonly used procedure consists of performing independent least-squares curve fittings to the real and imaginary pants of each component of the impedance matrix $\underline{H}$ over a range of frequencies. This procedure takes advantage of the fact that each system coefficient, $(M_{i,j},\ C_{i,j},\ K_{i,j})$, appears only in one impedance term making the polynomial curve fit (quadratic for the real part and linear for the imaginary part) independent of each other.

However, the direct least-squares curve fit of the system impedances is highly sensitive to the level of the inherent noise in the measurements and to the selection of the frequency range for the approximation *(8)*. A more robust method is achieved based on the following identity *(4)*

$$\underline{E}^k \underline{H}_{(\omega_k)} = I + E^k \qquad [7]$$

where $\underline{E}^k$ represents the measured flexibility matrix, defined as the inverse of the impedance $\underline{H}^k$, Eq. [6], at the frequency ω_k. $\underline{H}$ in the equation above corresponds to the estimated system impedance as defined by Eq. [3]. E^k is the matrix of errors due to the approximation. In this formulation, the flexibility coefficients work as weight functions of the errors in the minimization procedure. Whenever the flexibility coefficients are large, the error is also penalized by a larger value. As a result, the minimization procedure will become better in the neighborhood of the system resonances (natural frequencies) where the dynamic flexibilities are maximums (i.e., null dynamic stiffness, K-$\omega^2 M$). That is, the measurements containing resonance regions will have more weight on the fitted system parameters. This result is of importance since forcing functions exciting the system resonances are more reliable since this is more sensitive at those frequencies, and the measurements are accomplished with larger signal to noise ratios. In addition, it is precisely around the resonant frequencies where all the physical parameters (mass, damping and stiffness) most affect appreciably the system response. For "too low" frequencies the important parameter is the stiffness, while for "too high" frequencies the inertia dominates the response. Only near the resonance do all three parameters have an important effect on the system response. Therefore, it is more convenient to minimize the approximation errors using Eq. [7] rather than directly curve fitting the impedances. However, this last procedure could be rather intricate. The approximation functions on the left-hand-side of Eq. [7] are no longer independent of each other since all the parameters appear in all of them. This difficulty is easily overcome by rearranging the impedance definition Eq. [3] to the form

$$\underline{H}_{(\omega)} = \left[-\omega^2 I \,\vdots\, i\omega I \,\vdots\, I \right] \begin{bmatrix} \underline{M} \\ \underline{C} \\ \underline{K} \end{bmatrix} \qquad [8]$$

Substituting the definition Eq. [8] into Eq. [7] and separating into real and imaginary parts gives

$$\begin{bmatrix} Re\left(F^k \left[-\omega_k^2 I \,\vdots\, i\omega_k I \,\vdots\, I \right] \right) \\ Im\left(F^k \left[-\omega_k^2 I \,\vdots\, i\omega_k I \,\vdots\, I \right] \right) \end{bmatrix} = \begin{bmatrix} \underline{M} \\ \underline{C} \\ \underline{K} \end{bmatrix} = \begin{bmatrix} I \\ 0 \end{bmatrix} + \begin{bmatrix} Re\left(E^k \right) \\ Im\left(E^k \right) \end{bmatrix} \qquad [9]$$

Stacking the equations for the N discrete frequencies at which the identification procedure is to be performed renders

$$A \begin{bmatrix} \underline{M} \\ \underline{C} \\ \underline{K} \end{bmatrix} = \bar{I} + \bar{E} \qquad [10]$$

where

$$A=\begin{bmatrix}\begin{bmatrix}Re\left(\underline{F}^1\left[-\omega_1^2 I\,|\,i\omega_i I\,|\,I\right]\right)\\ Im\left(\underline{F}^1\left[-\omega_1^2 I\,|\,i\omega_1 I\,|\,I\right]\right)\end{bmatrix}\\ \begin{bmatrix}Re\left(\underline{F}^N\left[-\omega_N^2 I\,|\,i\omega_N I\,|\,I\right]\right)\\ Im\left(\underline{F}^N\left[-\omega_N^2 I\,|\,i\omega_N I\,|\,I\right]\right)\end{bmatrix}\end{bmatrix}\quad \bar{I}=\begin{bmatrix}\begin{bmatrix}I\\0\end{bmatrix}\\ \text{M}\\ \begin{bmatrix}I\\0\end{bmatrix}\end{bmatrix}\quad \bar{E}=\begin{bmatrix}\begin{bmatrix}Re\left(E^1\right)\\ Im\left(E^1\right)\end{bmatrix}\\ \text{M}\\ \begin{bmatrix}Re\left(E^N\right)\\ Im\left(E^N\right)\end{bmatrix}\end{bmatrix}$$

Fritzen *(3)* introduces the elegant Instrumental Variable Filter Method (IVF) to compute the system coefficients that minimize the Euclidean (L^2) norm of the global error matrix $\bar{E}$. This procedure was originally developed to estimate parameters in econometry problems. Massmann and Nordmann *(4)* have applied the method to fluid film seal elements. The IFV method proposes a solution of the form

$$\begin{bmatrix}M\\C\\K\end{bmatrix}^{m+1}=\left(\left[W^m\right]^T A\right)^{-1}\left[W^m\right]^T\bar{I} \qquad [11]$$

The weight matrix W is chosen to have the same form as A, see Eq. [10], but it consists of the analytical flexibilities rather than the measured ones, i.e.,

$$W^m=\begin{bmatrix}\begin{bmatrix}Re\left(\underline{F}^m_{(\omega_1)}\left[-\omega_1^2 I\,|\,i\omega_1 I\,|\,I\right]\right)\\ Im\left(\underline{F}^m_{(\omega_1)}\left[-\omega_1^2 I\,|\,i\omega_1 I\,|\,I\right]\right)\end{bmatrix}\\ \begin{bmatrix}Re\left(\underline{F}^m_{(\omega_N)}\left[-\omega_N^2 I\,|\,i\omega_N I\,|\,I\right]\right)\\ Im\left(\underline{F}^m_{(\omega_N)}\left[-\omega_N^2 I\,|\,i\omega_N I\,|\,I\right]\right)\end{bmatrix}\end{bmatrix} \qquad [12]$$

where

$$\underline{F}^m_{(\omega)}=\left[\left[-\omega^2 I\,|\,i\omega I\,|\,I\right]\begin{bmatrix}M\\C\\K\end{bmatrix}^m\right]^{-1} \qquad [13]$$

A first iteration (m=l) is performed with $W = A$, which corresponds to the standard least-squares solution of the problem in Eq. [10]. Then Eq. [11] is applied iteratively until a given convergence criterion is satisfied. This criterion can be conveniently chosen depending on the desired results. For example, the square summation of the differences between the parameters at iteration m and $(m\text{-}l)$ can be required to be less than a certain value, i.e. limiting the Euclidean norm of the error. Alternatively, it can be required that the largest difference be less than the largest acceptable error, i.e. limiting the L_1 norm of the error. Different tolerances to each variable could also be asserted depending on their physical units and significance. It is clear that the substitution of W for the discrete measured flexibility A (which also contains noise) improves the prediction of the system parameters. Note that the product A^TA amplifies the noisy components and adds them. Therefore, even if the noise has a zero mean value, the addition of its squares becomes positive resulting in a bias error. On the other hand, W does not have components correlated to the measurement noise. That is, no bias error is kept in the product W^TA. Consequently, the approximation to the system parameters is improved.

An example of the application of the IVF parameter identification method to a simple laboratory rotor-bearing system follows. Ransom, et al. *(9)* provides a successful application for the identification of force coefficients in multiple-pocket gas damper seals.

SFDs AND AIR ENTRAINMENT

Squeeze film dampers (SFDs) are effective means to introduce damping to rotor-bearing systems thus reducing vibration amplitudes at critical speeds and improving system stability. A SFD is a type of hydrodynamic bearing in which a non-rotating journal whirls with the shaft and squeezes a thin film of lubricant that surrounds it. The squeezing action generates hydrodynamic pressures yielding a force that opposes the journal motion and provides the desired damping. Generally, SFDs operate with low levels of external pressurization and are open to ambient on the sides. Under these conditions, the cyclic squeezing in and out of the oil results in the entrapment of external air and leads to the formation of a bubbly (foam-like) mixture of air and oil within the film *(10), (11)*. The mixture has different material properties than the pure lubricant, and consequently it affects considerably the dynamic force performance of the SFD. Zeidan, et al. *(12)* estimate damping coefficient losses as large as 75 percent of the value predicted for operation with pure oil.

The phenomenon of air entrainment is readily acknowledged to be the main obstacle for the reliable prediction of SFD dynamic forces *(13)*. Yet no accurate measurements correlating the viscous damping coefficients to the amount of entrained air are available. The lack of firm (quantifiable) experimental evidence prevents further advances in the theoretical formulation of SFD flows *(14), (15)*.

EXPERIMENTAL FACILITY

Figure 1 shows a section of the test rig and the instrumentation setup for force and displacements measurement. The shaft of length 305 mm (12") and diameter 9.5 mm (3/8") is supported by a bronze bushing at the drive end and by a squeeze film damper at the rotor midspan. The squeeze film damper consists of a steel journal of diameter (D) and length (L) equal to 50.8 mm and 25.4 mm, respectively, and a Plexiglas transparent housing. The damper radial clearance (c) is 0.29 mm (11.4 mils). Four flexible rods compose the squirrel cage that supports the damper journal. A ball bearing inside the SFD journal forces the shaft and the journal to whirl together while allowing the shaft to rotate. A flexible coupling transmits torque from the DC drive motor but isolates lateral vibration. A massive disk is mounted on the free end of the shaft to provide inertia and a location to install imbalance masses.

Two eddy current proximity sensors measuring horizontal and vertical shaft displacements are installed at (L_x) 213 mm and (L_Y) 254 mm from the rotor drive end, respectively. The SFD and disk centers are located at (L_{SFD}) 151 mm and (L_D) 274 mm from the

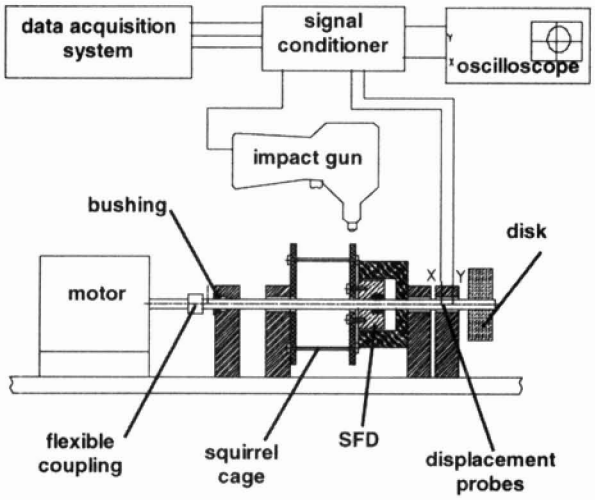

Fig. 1—Test rig section and instrumentation.

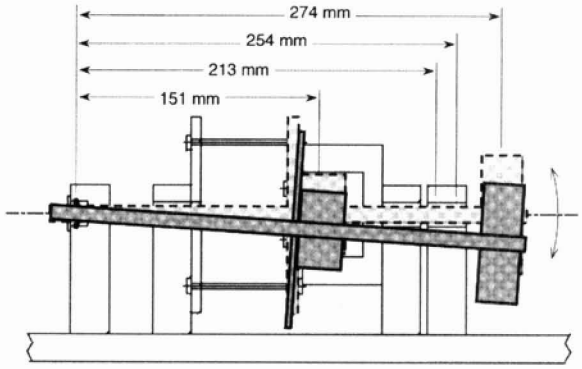

Fig. 2—Conical mode shape of the rotor

rotor drive end, respectively. The bushing stiffness is larger than the SFD elastic support stiffness, and thus the rotor pivots about the bushing location for rotor speeds below 6000 rpm as shown in Fig. 2. For the range of frequencies of interest, the rotor can be considered as an equivalent point mass system with two degrees of freedom in the lateral directions (X, Y).

A controlled mixture of air and ISO VG 2 oil flows to the SFD through a small hole located at the top of the bearing housing. The viscosity (μ) of the pure lubricant is 2.25 centipoise at a temperature of 30°C. The lubricant exits the test section through both sides of the damper which are open to ambient. The mixture is generated in a sparger element installed at the connection of the air and oil lines. The proportions of air and oil are accurately regulated with valves on each feed line. The air volume fraction is computed as the ratio of measured air volumetric flow rate to total (air + oil) volumetric flow rate.

An instrumented impact gun excites the rotor shaft at the location of the SFD. A support allows installation of the impact gun for excitations in the horizontal and vertical directions. An A/D board and computer record the time traces of the impact force and the shaft lateral displacements simultaneously at a rate of 6700 samples per second for 1.2 seconds. All tests are performed without rotor spinning.

EXPERIMENTAL PROCEDURE

The rotor is carefully centered within the damper clearance and the valves in the oil and air feed lines are set to the desired mixture composition. The air and oil flow rates as well as the values of supply pressures and temperature are recorded for the computation of the air volume fraction. The system fundamental natural frequencies, measured by impact tests under dry conditions, are equal to 28.4 Hz and 30.1 Hz in the horizontal and vertical directions, respectively. The difference is due to asymmetry in the squirrel cage stiffness as demonstrated earlier by static load measurements of the system flexibility *(15)*.

The test system has two DOF (n=2). Thus, two independent excitations are required to compute all four coefficients of the impedance matrix $\underline{H}$. Impact loads in the horizontal (X) and vertical (Y) directions are sufficient to perform the identification procedure. Eight impacts are exerted on each direction for every mixture condition, and the time traces of forces and displacements are stored. The impact forces are applied at the SFD journal and the shaft displacements are measured near the end disk. Equivalent X and Y displacements at the SFD location are computed using the conical mode of motion with a pivot at the bushing as depicted in Fig. 2. A DFT transform is applied to the dynamic displacements and loads, and the resulting spectra are regrouped into eight sets, each one containing the data from the X and Y impacts. Equation [6] is then employed to compute the impedance elements ($\underline{H}_{XX}$, $\underline{H}_{XY}$, $\underline{H}_{YX}$, $\underline{H}_{YY}$) for each data set at the discrete values of frequency. Then, the eight discrete functions corresponding to each impedance coefficient are averaged to render a single frequency function in which the noise not related to the load excitation is reduced. Note that using the average of the impedance and/or flexibility (transfer) functions, instead of computing the transfer function from frequency averaged responses and excitations, eliminates the requirement for repetitive excitations thus allowing for the use of hand-held impact hammers or the combination of different types of excitations. Figure 3 shows typical time variations of the applied force and displacement responses, and their corresponding DFTs for one case of impact excitation in the X direction. The measurements include a short pre-trigger and contain the full span of the transient motions, thus avoiding "leaking" effects on the DFT transforms. Figure 3 also shows the excitation to have a wide-band spectrum that covers the whole range of frequencies of interest.

The IVF parameter identification method, Eq. [11], is applied to the averaged flexibilities over a selected range of frequencies around the fundamental natural frequency of the system. In this case, the selected range goes from 8.1 Hz to 48.8 Hz and includes the peak response (resonance) region. The process is repeated for six different lubricant mixture compositions ranging from pure oil to 100 percent air. The IVF identification process renders estimates for the system force coefficients $(M_{ij}, C_{ij}, \text{and } K_{ij})_{i,j=X,Y}$ as functions of the air volume content in the mixture. These are equivalent system parameters referred to the location of the SFD middle plane.

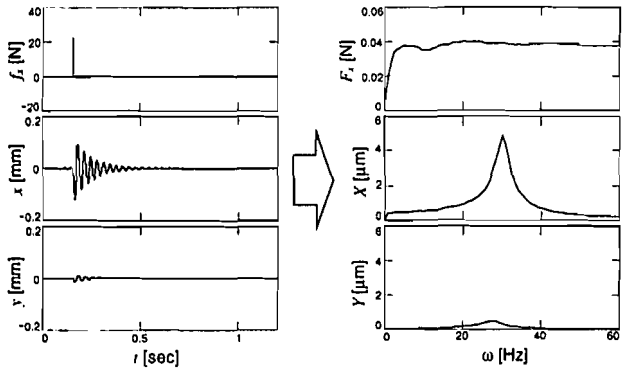

Fig. 3—Typical impact excitation in the X direction and response displacements (X and Y) in time and frequency domains.

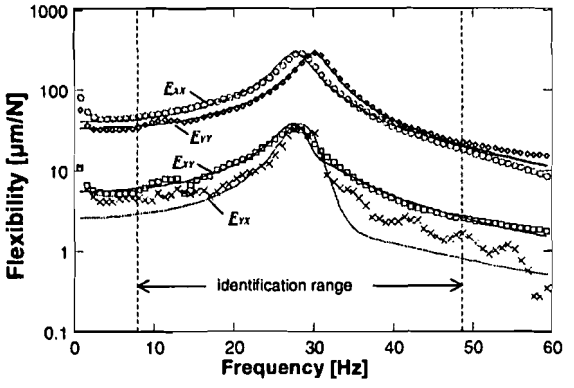

Fig. 4—Measured and approximated system flexibilities. Air volume fraction = 8.6%.

TEST RESULTS

Figure 4 depicts with symbols the flexibilities $(\underline{E}_{ij})_{i,j=X,Y}$ measured for an air/oil mixture volume content of 8.6 percent as a function of the excitation frequency. The continuous lines represent the flexibilities calculated with the estimated system parameters. The experimental values represent the averages from multiple impacts as discussed before. Note that the cross-coupled flexibilities are at least one order of magnitude lower than the direct system flexibilities. Correlations between the measurements and the analytical (curve fit) functions are computed for each direct and cross-coupled flexibilities to provide a measure of the goodness of the approximation. All correlations range between 94 percent and 98 percent demonstrating the effectiveness of the IVF method. Furthermore, the coherence of the direct displacements to the exerted loads shows values near unity for the range of frequencies considered.

Figures 5 through 7 depict the estimated dynamic force coefficients acting at the damper location. The values for an air volume fraction of one, i.e. pure air or "dry" condition, represent solely the effect of the support structure and rotor inertia without any influence of the squeeze film. These coefficients, identified earlier by other means, serve to validate the dynamic measurement process and identification method. The direct inertia coefficients

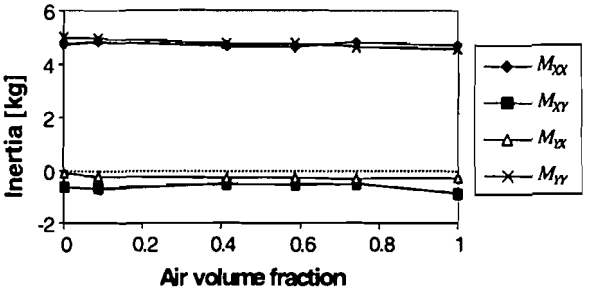

Fig. 5—Equivalent inertia coefficients *vs.* air volume fraction.

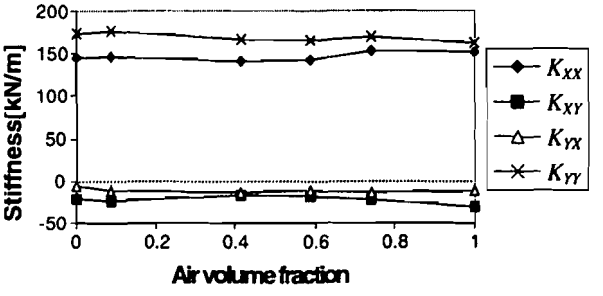

Fig. 6—Equivalent stiffness coefficients *vs.* air volume fraction.

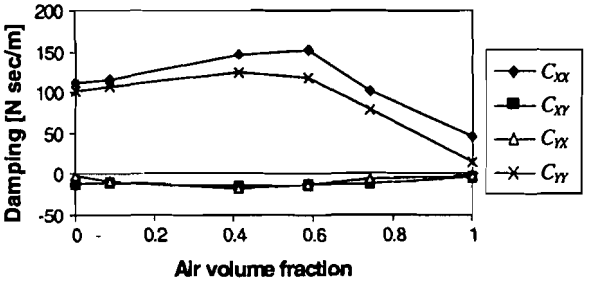

Fig. 7—Equivalent damping coefficients *vs.* air volume fraction.

are determined by weighing the shaft, disk and journal and using simple geometrical relations to evaluate the equivalent inertia at the SFD location. The value calculated by this procedure is 4.02 kg, and somewhat lower than the magnitudes identified from the dynamic response tests. The direct stiffness of the elastic damper support in the horizontal direction (K_{XX}) is determined by applying static loads with a dynamometer and recording displacements with a dial gauge indicator. The measured value is K_{XX} = *ISO kN/m*. The equivalent structural damping is estimated from the logarithmic decrement of the dynamic response to an impact. The direct damping coefficient for no lubricant is estimated as 22.3 N.s/m.

Figure 5 shows the direct and cross-coupled inertia coeffi-

cients estimated by the IVF method as a function of the mixture air volume fraction. At a volume fraction of one, i.e., pure air, the IVF method confirms the estimations of mass coefficients performed by weighing the parts. The results also show that no significant fluid inertia is introduced by the SFD since the system direct inertia coefficients (M_{XX}, M_{YY}) remain invariant when oil flows through the damper lands. The cross-coupled inertia coefficients (M_{XY}, M_{YX}) are nearly null in all test cases.

The estimated IVF stiffness coefficients $[K_{ij}]_{i,j=X,Y}$ are depicted in Fig. 6 for air volume fractions ranging from zero (pure oil) to one (pure air). The measurements for the "dry" condition confirm the static measurements of the structure characteristics. No appreciable change is observed in any of the stiffness coefficients (direct or cross-coupled) when oil is fed to the damper. The cross-coupled stiffnesses are nearly zero, though definitely negative in all tests. The vertical direct stiffness is slightly larger than the horizontal one, which agrees with the higher natural frequency measured in the vertical direction.

The average values and maximum percent variation for the stiffness and inertia force coefficients are:

K_{XX} = 146.3kN/m(4.3%), K_{YY} = 169.1 kN/m(4.1%),
K_{XY} = 22.3 kN/m (38.7%), K_{YX} = 11.5 kN/m (24.2%),
M_{XX} = 4.7 kg (2.3%), M_{YY} = 4.8 kg (3.1%),
M_{XY} = 0.62 kg (43.4%), M_{YX} = 0.25 kg (52.4%),

Figure 7 depicts the variation of the system damping coefficients $[C_{ij}]_{i,j=X,Y}$ as the air volume content in the mixture increases. The measurements of the "dry" direct damping coefficients coincide with the preliminary tests based on the system logarithmic decrement. Predicted values of the SFD damping coefficients for the pure oil condition, centered journal and a full film extent are equal to *(17)*

$$C_{XX} = C_{YY} = 12\pi\mu R\left[\frac{L}{c}\right]^{-3}\left(1-\frac{tgh(L/D)}{(L/D)}\right) = 100 N.s/m$$
$$C_{XY} = C_{YX} = 0 \qquad [14]$$

These values are very close to the identified viscous damping coefficients. The estimated test cross-coupled damping coefficients are rather small, most likely within the uncertainty of the measurements. As expected, the direct damping coefficients (C_{XX}, C_{YY}) vary significantly with the air/oil mixture composition. However, contrary to expected results, the direct damping coefficients increase steadily as the air volume fraction rises to a mixture with 50 percent air content. For larger concentrations of air/oil volume the direct damping coefficients decrease rapidly towards their "dry" value.

The unusual damping coefficients identified imply an increase in the effective viscosity of the lubricant mixture for small air volume contents. Chamniprasart, et al. *(18)* provide a fundamental analysis and limited empirical evidence verifying this phenomenon. The present authors speculate that the nature of the impact tests generates too fast system transient responses which may prevent the mixture compressibility from affecting the generation of squeeze film pressures or the overall damping coefficients. It may also be possible that, since the SFD is open to ambient on both sides, the air in the mixture is expelled from the film earlier than the oil, thus resulting in a lubricant with a lower air content than the one measured in the supplied mixture.

Diaz and San Andres *(8), (14), (15)* detail measurements of damping coefficients in a SFD performing sustained circular centered orbital motions at various whirl frequencies. In these experiments, the SFD force coefficients steadily decrease as the air content increases in the lubricant mixture. These references reveal the complexity in the structure of bubbly flow fields and their effects on SFD force performance.

CONCLUSIONS

The instrumental variable filter (IVF) method proves a reliable tool for the identification of bearing force coefficients. The general formulation presented easily allows for extension of the method to account for support flexibility or even shaft flexibility when the equations of motion of a system need to be established experimentally. Application of the IVF renders the inertia, stiffness, and damping matrices of a linear system according to the selected degrees of freedom. However, the selection of the appropriate degrees of freedom is not always evident, thus representing the most critical pant of the parameter identification process. The excitation force employed is also an important factor. Many options are available, but the impact force stands out because of the ease of its implementation and its wide frequency spectrum.

The IVF method is applied to the identification of system force coefficients in a small test rotor supported on a squeeze film damper (SFD) lubricated with a mixture of air in oil. The measurements show that the SFD does not introduce any significant amount of stiffness or inertia to the structural system. The cross-coupled damping coefficients are also negligible in all test cases. A curious trend is unveiled for the direct damping coefficients (C_{XX}, C_{YY}). Instead of a monotonic decrease for increasing air volume fractions, the direct damping coefficients increase slightly up to a lubricant composition of about 50 percent air in volume, where they reach a maximum. Further increase of air content reduces the damping coefficients until they reach the "dry" damping value for a pure air condition. The present results confirm that the amount of damping provided by a SFD is greatly affected by air entrainment. However, it is suspected that the increased viscosity for low air volume fractions will not be enough to produce an increment of the actual damping in an operating SFD with sustained whirl motions of significant amplitude and where the mixture compressibility effect is of utmost importance.

ACKNOWLEDGMENTS

The support of the National Science Foundation is gratefully acknowledged. The first author also acknowledges the support of CONICIT (Consejo Nacional de Investigaciones Científicas y Tecnológicas) and Universidad Simón Bolívar, Venezuela. Thanks to Mr. C. W. Karstens, undergraduate student, who performed most of the experimental work.

REFERENCES

(1) Robinson, M., Arauz, G. and San Andrés, L., "A Test Rig for the Identification of Rotordynamic Force Coefficients of Fluid Film Bearing Elements," ASME Paper **95-GT-431**, (1995).

(2) Ransom, D. L., "Identification of Dynamic Force Coefficients of a Labyrinth and Gas Damper Seal Using Impact Load Excitations," Master Thesis, Texas A&M University, December, (1997).

(3) Fritzen, C., "Identification of Mass, Damping, and Stiffness Matrices of Mechanical Systems," ASME Paper **85-DET-91**, (1985).

(4) Massmann, H. and Nordmann, R., "Some New Results Concerning the Dynamic Behavior of Annular Turbulent Seals," **NASA CP 2409**, in *Proc. of the Instability in Rotating Machinery Workshop*, Carlson City, pp 179-194, (1985).

(5) Muller-Karger, C. M. and Granados, A. L., "Derivation of Hydrodynamic Bearing Coefficients Using the Minimum Square Method," *ASME Jour. of Trib.*, **119**, 4, pp 802-807, (1997).

(6) Diaz, S. E. and San Andrés, L. A., "Measurements of Pressure in a Squeeze Film Damper with an Air/Oil Bubbly Mixture," *Trib. Trans.*, **411**, 2, pp 282-288, (1998).

(7) Rouvas, C., "Parameter Identification of the Rotordynamic Coefficients of High-Reynolds-Number Hydrostatic Bearings," Ph.D. Dissentation, Texas A&M University, College Station, TX, (1993).

(8) Diaz, S. E., "Experimental Parameter Identification of a nxn Linear System," Internal Research Progress Report, Rotordynamics Laboratory, Texas A&M University, College Station, TX, (1997).

(9) Ransom, D., Li, J., San Andrés, L. and Vance, J. M., "Experimental Force Coefficients for a Two-Bladed Labyrinth Seal and a Four-Pocket Damper Seal," ASME Paper **98-Trib-28**, (1998).

(10) Walton, J., Walowit, J., Zorzi, E. and Schrand, J., "Experimental Observation of Cavitating Squeeze Film Dampers," *ASME Jour. of Trib.*, **109**, pp 290-295, (1987).

(11) Zeidan, F. Y. and Vance, J. M., "Cavitation Leading to a Two Phase Fluid in a Squeeze Film Damper," *Trib. Trans.*, **32**, 1, pp 100-104, (1989).

(12) Zeidan, F. Y., Vance, J. M. and San Andrés, L. A., "Design and Application of Squeeze Film Dampers in Rotating Machinery," in *Proc. of the 25th Turbomachinery Symp.*, Texas A&M University, College Station, TX, pp 169-188, (1996).

(13) Childs, D., *Turbomachinery Rotordynamics*, John Wiley & Sons, NY, (1993).

(14) Diaz, S. and San Andrés, L., "Reduction of the Dynamic Load Capacity in a Squeeze Film Damper Operating with a Bubbly Lubricant," ASME Paper **98-GT-109**, (1998).

(15) Diaz, S. and San Andrés, L., "Effects of Bubbly Flow on the Dynamic Pressure Fields of a Test Squeeze Film Damper," ASME Paper **FEDSM98-5070**, in *Proc. of the 1998 ASME Fluids Engineering Division Summer Meeting*, Washington, DC, June, (1998).

(16) Karstens, C. W., "Effects of Air Entrainment on the Damping Coefficients of a Squeeze Film Damper," Senior Honor Thesis, Texas A&M University, (1997).

(17) San Andrés, L. and Vance, J., "Effect of Fluid Inertia on Squeeze Film Damper Forces for Small Amplitude Circular Centered Motions," *ASLE Trans.*, **30**, pp 69-76, (1987).

(18) Chamniprasart, K., Al-Sharif, A., Rajagopal, K. R. and Szeri, A. Z., "Lubrication With Binary Mixtures: Bubbly Oil," *ASME Jour. of Trib.*, **115**, pp 253 - 260, (1993).